Nit1 is a metabolite repair enzyme that hydrolyzes deaminated glutathione

Alessio Peracchi[a,b,c,1,2,3,4], Maria Veiga-da-Cunha[a,b,3,4], Tomiko Kuhara[d,e], Kenneth W. Ellens[f], Nicole Paczia[f], Vincent Stroobant[g], Agnieszka K. Seliga[a,b], Simon Marlaire[a,b], Stephane Jaisson[a,b,5], Guido T. Bommer[a,b], Jin Sun[h], Kay Huebner[h], Carole L. Linster[f], Arthur J. L. Cooper[i], and Emile Van Schaftingen[a,b,4]

[a]Walloon Excellence in Lifesciences and Biotechnology, B-1200 Brussels, Belgium; [b]de Duve Institute, Université Catholique de Louvain, B-1200 Brussels, Belgium; [c]Department of Life Sciences, Laboratory of Biochemistry, Molecular Biology, and Bioinformatics, University of Parma, 43124 Parma, Italy; [d]Japan Clinical Metabolomics Institute, Kahoku, Ishikawa 929-1174, Japan; [e]Human Genetics, Medical Research Institute, Kanazawa Medical University, Uchinada, Ishikawa 920-0293, Japan; [f]Luxembourg Centre for Systems Biomedicine, Université du Luxembourg, L-4367 Belvaux, Luxembourg; [g]Ludwig Institute for Cancer Research, de Duve Institute, Université Catholique de Louvain, B-1200 Brussels, Belgium; [h]Department of Cancer Biology and Genetics, Ohio State University, Columbus, OH 43210; and [i]Department of Biochemistry and Molecular Biology, New York Medical College, Valhalla, NY 10595

Edited by Shelley D. Copley, University of Colorado, Boulder, CO, and accepted by Editorial Board Member Stephen J. Benkovic March 9, 2017 (received for review August 17, 2016)

The mammalian gene *Nit1* (nitrilase-like protein 1) encodes a protein that is highly conserved in eukaryotes and is thought to act as a tumor suppressor. Despite being ∼35% sequence identical to ω-amidase (Nit2), the Nit1 protein does not hydrolyze efficiently α-ketoglutaramate (a known physiological substrate of Nit2), and its actual enzymatic function has so far remained a puzzle. In the present study, we demonstrate that both the mammalian Nit1 and its yeast ortholog are amidases highly active toward deaminated glutathione (dGSH; i.e., a form of glutathione in which the free amino group has been replaced by a carbonyl group). We further show that *Nit1*-KO mutants of both human and yeast cells accumulate dGSH and the same compound is excreted in large amounts in the urine of *Nit1*-KO mice. Finally, we show that several mammalian aminotransferases (transaminases), both cytosolic and mitochondrial, can form dGSH via a common (if slow) side-reaction and provide indirect evidence that transaminases are mainly responsible for dGSH formation in cultured mammalian cells. Altogether, these findings delineate a typical instance of metabolite repair, whereby the promiscuous activity of some abundant enzymes of primary metabolism leads to the formation of a useless and potentially harmful compound, which needs a suitable "repair enzyme" to be destroyed or reconverted into a useful metabolite. The need for a dGSH repair reaction does not appear to be limited to eukaryotes: We demonstrate that Nit1 homologs acting as excellent dGSH amidases also occur in *Escherichia coli* and other glutathione-producing bacteria.

metabolite repair | deaminated glutathione | amidase | aminotransferases

Genome sequencing has led to the identification of numerous proteins sharing significant sequence identity with enzymes, but whose catalytic activity remains to be established. Knowing the function of these putative enzymes, particularly if they are highly conserved, may reveal important aspects of intermediary metabolism that have remained unexplored until now. The purpose of the present work was to determine the catalytic role of nitrilase-like protein 1 (Nit1), a highly conserved protein with still unknown function (1–6) but homologous to Nit2 (ω-amidase) (5, 6), an enzyme whose activity is closely linked to transamination reactions.

In fact, aminotransferases that use L-glutamine as a substrate yield, as a product, the corresponding ketoacid, α-ketoglutaramate (α-KGM) (Fig. 1*A*). Such a reaction is rendered metabolically irreversible by the coupled activity of ω-amidase, which hydrolyzes α-KGM to α-ketoglutarate (α-KG) and ammonia (Fig. 1*A*) (7–9). In mammals, ω-amidase is encoded by the *Nit2* gene (5, 6).

In addition to *Nit2*, the genomes of the most evolved eukaryotes contain almost invariably the gene *Nit1*, whose product shows ∼35% sequence identity with Nit2. Compared with Nit2, however, the Nit1 protein shows only weak ω-amidase activity toward α-KGM (catalytic efficiency <0.1% of that of Nit2) (5). The observation that in many invertebrates Nit1 is expressed as a domain fused with a fragile histidine triad protein (Fhit, suggested to act as a tumor suppressor in mammals) (1), has fueled a substantial interest in deciphering the physiological substrates of this enzyme. Galperin and Koonin even included *Nit1* among the "top 10" most attractive targets for functional assignment (10, 11), assuming that clarification of its activity could illuminate new aspects of biology. Despite all this interest, the actual enzymatic function of Nit1 has so far remained elusive.

Sequence comparisons and structural data indicate that the residues of the Nit2 catalytic pocket that surround the substrate α-KGM are conserved in Nit1. A major difference is, however,

Significance

The genomes of the vast majority of eukaryotes encode a protein [named nitrilase-like protein 1 (Nit1) in humans and mice] whose enzymatic function has long been unknown. We show here that the mammalian Nit1 and the corresponding yeast protein efficiently hydrolyze the deaminated form of the common intracellular antioxidant glutathione. In turn, deaminated glutathione can be produced by a side activity of numerous transaminases. Thus, Nit1 repairs an undesired product, arising from the slow (and erroneous) transformation of an important metabolite by some abundant intracellular enzymes. The importance of this Nit1 function is underscored by the finding that enzymes with the same activity occur in *Escherichia coli* and in other glutathione-producing bacteria.

Author contributions: A.P., M.V.-d.-C., and E.V.S. designed research; A.P., M.V.-d.-C., T.K., K.W.E., N.P., V.S., A.K.S., S.M., S.J., G.T.B., and C.L.L. performed research; J.S. and K.H. contributed new reagents/analytic tools; A.P., M.V.-d.-C., T.K., K.W.E., N.P., V.S., A.K.S., S.M., S.J., G.T.B., C.L.L., A.J.L.C., and E.V.S. analyzed data; and A.P. and E.V.S. wrote the paper.

The authors declare no conflict of interest.

This article is a PNAS Direct Submission. S.D.C. is a guest editor invited by the Editorial Board.

Freely available online through the PNAS open access option.

[1]A.P. mainly contributed to the present research while on sabbatical leave at the de Duve Institute, Université Catholique de Louvain.

[2]Present address: Department of Chemistry, Life Sciences, and Environmental Sustainability, University of Parma, 43124 Parma, Italy.

[3]A.P. and M.V.-d.-C. contributed equally to this work.

[4]To whom correspondence may be addressed. Email: alessio.peracchi@unipr.it, maria.veiga@uclouvain.be, or emile.vanschaftingen@uclouvain.be.

[5]Present address: Laboratory of Paediatric Biology and Research, University Hospital of Reims, Maison Blanche Hospital, 51092 Reims, France.

This article contains supporting information online at www.pnas.org/lookup/suppl/doi:10.1073/pnas.1613736114/-/DCSupplemental.

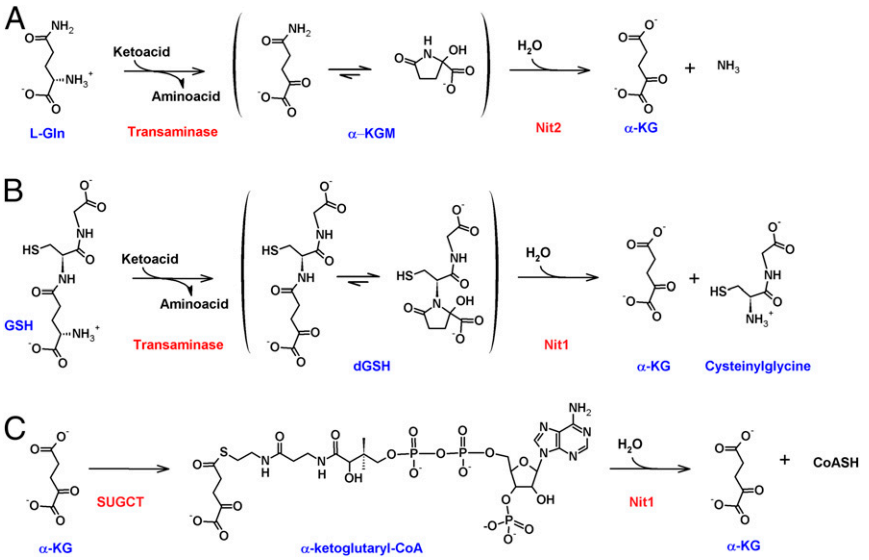

Fig. 1. The Nit2 reaction and the working hypotheses tested in this work about Nit1 activity. (*A*) The known coupled reactions catalyzed by glutamine transaminases and ω-amidase (Nit2). The transamination of glutamine yields α-KGM, the linear form of which equilibrates with a cyclic form (two potential anomers). Nit2 catalyzes the hydrolysis of the open form to α-KG and ammonia. (*B*) An analogous process, in which the transamination of GSH to dGSH is followed by hydrolysis of dGSH to α-KG and cysteinylglycine. (*C*) α-KG–CoA, formed by SUGCT (C7orf10), is another potential substrate for Nit1.

found in the subsite where the amido group of α-KGM is predicted to bind, which is a quite small niche in the structure of Nit2, but a much larger cavity in Nit1 (2, 4). These structural features suggest that Nit1 serves to hydrolyze an α-KG or α-KGM derivative attached to a rather large structure. Because no classic reaction of intermediary metabolism leads to the formation of such compounds, we considered the possibility that nonclassic compounds could be formed by side reactions of classic enzymes of intermediary metabolism and that Nit1 would serve as a "metabolite repair" enzyme.

Recent research has unveiled the importance of metabolite repair in intermediary metabolism (12, 13). According to this concept, enzymes of intermediary metabolism are not perfectly specific and tend to act on intracellular compounds resembling their true substrate. The products of these side reactions are nonclassic metabolites, which in several cases need to be eliminated or recycled by specific enzymes, called metabolite repair enzymes (12). Deficiency in such enzymes causes accumulation of the "abnormal" metabolite and may lead to disease, as in the case of L-2-hydroxyglutaric aciduria (14, 15) or to major metabolic perturbations because of enzyme inhibition (16). The increasing rate at which repair enzymes are being discovered suggests that a substantial fraction of currently "unclassified" enzymes (17), encoded in eukaryotic and prokaryotic genomes, could play a role in metabolite repair.

Conceivably, at least two types of reactions might lead to the formation of bulky ω-derivatives of α-KG: (*i*) transamination reactions leading to the conversion of glutathione (GSH) to a deaminated form (called deaminated GSH or dGSH in the present work) (Fig. 1*B*); and (*ii*) the "erroneous" attachment of a CoA group to α-KG by succinyl-CoA:glutarate-CoA transferase (SUGCT), which would lead to α-ketoglutaryl–CoA (α-KG–CoA) (Fig. 1*C*). Our purpose was to test these compounds as substrates for Nit1. In this work, we provide evidence that mouse Nit1 (mmNit1) and its *Saccharomyces cerevisiae* ortholog (scNit1; see Table 1 for the designation of the proteins investigated in the present work) are excellent dGSH amidases and that their inactivation leads to the accumulation of dGSH in cell models as well as in vivo.

Results

Nit1 Efficiently Hydrolyzes the Amide Bond in dGSH. dGSH and deaminated ophthalmic acid (dOA)—OA is a physiological tripeptide analog of GSH where the central cysteine is replaced by 2-aminobutyrate, a cysteine structural analog unable to form disulfides—as well as α-KGM, were prepared by oxidation of the appropriate compounds with snake venom L-amino acid oxidase, an enzyme that displays broad specificity (18, 19), and subsequently separated from the parent compound by cation-exchange chromatography (5). When dGSH and dOA were further purified by reverse-phase HPLC, both compounds eluted in two

Table 1. Proteins investigated in the present work

Species	Gene reference (DOE website)	Gene symbol	Protein designation
Mus musculus	639390753	*Nit1*	mmNit1
	639398620	*Nit2*	mmNit2
Saccharomyces cerevisiae	638211686	*NIT2*	scNit1
	638212758	*NIT3*	scNit2
Escherichia coli	646917127	*ybeM (ybl23)*	ecYbeM
	646916767	*yafV*	ecYafV
Yersinia enterocolitica	2638510043	*y0194*	yeNit1
	2638509534	No gene symbol	yeYafV
Pseudomonas aeruginosa	2687301550	*PA4475*	paNit1
	2687297946	*PA3797*	paYafV
Synechocystis sp. *GT-S, PCC6803*	651080170	*sll0601*	syNit1
Bifidobacterium longum	2650840504	No gene symbol	blYbeM
Staphylococcus aureus	2511961111	*amiE*	saYafV

Genes and protein sequences can be retrieved from the Department of Energy (DOE) website (https://img.jgi.doe.gov/cgi-bin/mer/main.cgi). The designations for the bacterial proteins studied in this work other than *E. coli* have been chosen based on their degree of identity with the mouse or *E. coli* proteins (see *SI Appendix*, Fig. S14 and Table S3). For example, blYbeM shows a higher degree of identity with ecYbeM than with mmNit1, mmNit2, or ecYafV; similarly, paNit1 shows a higher degree of identity with mmNit1 than with mmNit2, ecYbeM or ecYafV.

different peaks, corresponding to the two anomeric forms of the cyclized ketoacid. A peak attributable to the linear form was not detectable, suggesting that, in analogy with the case of α-KGM (20), such a linear form is largely unfavored for dGSH and dOA. dGSH, in addition to the two anomeric peaks, presented additional peaks eluting later and corresponding to disulfides of dGSH with GSH and with itself. Such additional peaks disappeared if the sample was treated with excess DTT before chromatography.

After purification, dGSH and dOA were tested as substrates for the recombinant mouse enzymes (mmNit1 and mmNit2) and for their yeast homologs, using a coupled assay with glutamate dehydrogenase (GDH) that monitors the release of α-KG. As shown in Table 2 and its legend, both dGSH and dOA are good substrates for mmNit1 and scNit1, whereas α-KGM is a much poorer substrate. Conversely, mmNit2 and its yeast counterpart acted efficiently on the small substrate α-KGM but showed no detectable activity toward the larger substrates derived from GSH and OA.

Having established that the Nit1 activity releases α-KG from dGSH and dOA, we also tested whether the other products of these reactions are, respectively, cysteinylglycine and 2-aminobutyrylglycine, as expected. Generation of stoichiometric amounts of 2-aminobutyrylglycine from dOA was demonstrated by *N*-labeling the reaction mixture with 6-aminoquinolyl-*N*-hydroxysuccinimidyl carbamate (AQC) and identifying the AQC-derivative of the dipeptide by reverse-phase HPLC (*SI Appendix*, Fig. S1). For unknown reasons, we were unable to detect the second product of dGSH cleavage by this method, but could easily measure the formation of cysteinylglycine directly in the reaction mixture, exploiting its known propensity to form a thiazolidine adduct with pyridoxal 5′-phosphate (PLP) (21). Because the formation of this adduct requires the presence of both a free amino group and of a free thiol on the same molecule (21), this technique confirmed that cysteinylglycine was formed in stoichiometric amounts during dGSH cleavage (*SI Appendix*, Fig. S2).

It is well established that ω-amidase acts on the linear form of α-KGM (20), despite the fact that in solution this form is 300-fold less abundant than the cyclic (lactam) forms (Fig. 1*A*). Because substituted derivatives of α-KGM also tend to cyclize, we tested the effect of increasing mmNit1 concentrations on the rate of dGSH hydrolysis. The measured reaction rate leveled off at high enzyme concentration, implying that under those conditions opening of the cyclic form becomes rate-limiting for the whole process (*SI Appendix*, Fig. S3*A*). From this experiment, we inferred an apparent first-order rate constant for ring opening of 0.26 min^{-1} at pH 7.2. By comparison, at the same pH, opening of the α-KGM form occurs with an apparent first-order rate constant of 0.0011 min^{-1} (20). This difference is likely attributable to internal catalysis because of the presence of the thiol group and of the glycine carboxylic group in dGSH. Consistent with this interpretation, the corresponding opening of cyclic dOA appears to be about 10-fold slower compared with dGSH (*SI Appendix*, Fig. S3*B*).

With this information in hand, we designed experiments to measure the catalytic parameters exhibited by mmNit1 and its yeast ortholog (scNit1) under conditions where the opening of the cyclic form is not rate limiting. As shown in Table 2, the apparent catalytic efficiencies (k_{cat}/K_M) toward dGSH for mmNit1and scNit1 are in the range 10^4 to 10^5 $M^{-1}\cdot s^{-1}$, over 1,000-fold higher than those observed toward α-KGM. These apparent k_{cat}/K_M values are also close to the "average" value for metabolic enzymes (22). If one considers that the actual substrate of these amidases is in fact the (minimally abundant) linear form of dGSH, as shown above, the "correct" k_{cat}/K_M values for mmNit1 and its yeast counterpart should greatly exceed 10^6 $M^{-1}\cdot s^{-1}$.

dGSH Accumulates in *Nit1*-Deficient Model Cells and in the Urine of *Nit1*-KO Mice. We prepared human cell lines (HAP1) deficient in Nit1 and Nit2 by CrispR/Cas9 technology. We selected two distinct *Nit1*-KO clones, targeted at two locations of the *Nit1* gene by using different guide RNAs, as described in *Materials and Methods*. Sequencing of the DNA indicated the presence of mutations incompatible with the production of an active Nit1 protein in these clones (*SI Appendix*, *Supplementary Materials and Methods*). Analysis of cell extracts by liquid chromatography-mass spectrometry (LC/MS) indicated the presence of a peak with the same exact *m/z* ratio and elution volume as dGSH (*SI Appendix*, Fig. S4*A*). Analysis of samples derived from cells deficient in Nit2 or from control cells revealed much lower amounts of the same compound. Assuming a water cell volume of 2.5 μL/mg protein, we estimated that the intracellular dGSH

Table 2. Observed rates and catalytic parameters for the reactions catalyzed by recombinant mouse Nit1 and Nit2 and by their yeast orthologs

α-KGM or dGSH	Activity at 80 μM substrate (μmol·min^{-1}·mg^{-1})	V_{max}* (μmol· min^{-1}·mg^{-1})	k_{cat} (s^{-1})	K_M (μM)	k_{cat}/K_M ($M^{-1}\cdot s^{-1}$)
α-KGM					
mmNit1	$2.6 \times 10^{-3} \pm 3 \times 10^{-4}$	—	—	—	18 ± 2†
scNit1	$1.5 \times 10^{-3} \pm 2 \times 10^{-4}$	—	—	—	12 ± 2†
mmNit2	4.3 ± 0.5	19.4 ± 1.4	10.7 ± 0.7	250 ± 40	43,000 ± 3,000
scNit2	1.6 ± 0.23	40.2 ± 1.5	23.5 ± 0.9	1,600 ± 200	14,700 ± 2,100
dGSH					
mmNit1	0.8 ± 0.05	2.6 ± 0.4	1.6 ± 0.3	170 ± 60	9,400 ± 3,000
scNit1	2.7 ± 0.5	5.8 ± 0.5	3.6 ± 0.3	45 ± 6	80,000 ± 12,000
mmNit2	$\leq 3 \times 10^{-4}$	—	—	—	<3
scNit2	$\leq 1.6 \times 10^{-4}$	—	—	—	<2

Values are the average (± SEM) of at least three separate measurements. Activities were determined at pH 8.5 (30 °C) and at enzyme concentrations calibrated to ensure that the spontaneous opening of the cyclic forms of the substrates was not rate-limiting for the reaction measured. Details are provided in *Materials and Methods*. Activities (μmol·min^{-1}·mg^{-1}) toward 80 μM dOA were 0.07 ± 0.01 (mmNit1), 0.85 ± 0.03 (scNit1), $\leq 2 \times 10^{-4}$ (mmNit2) and $\leq 3 \times 10^{-4}$ (scNit2).

*Specific activity at saturating concentration of substrate.

†k_{cat}/K_M corresponds to the initial slope of the Michaelis-Menten hyperbola. Because the activities of both mmNit1 and scNit1 toward α-KGM increased linearly with substrate concentration up to at least 80 μM, k_{cat}/K_M values were estimated from the slopes of such increases. Because of the very low activity of mmNit1 and scNit1 with α-KGM, enzyme concentrations in these experiments were in the 0.5–1.5 μM range.

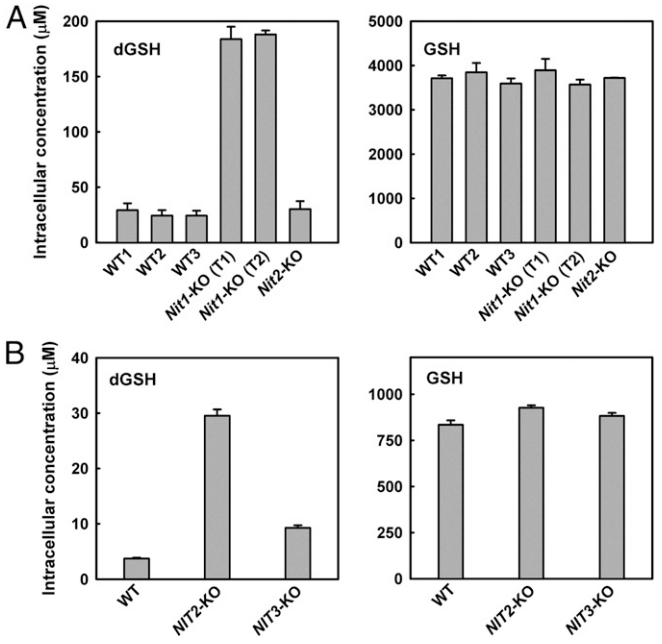

Fig. 2. Accumulation of dGSH in *Nit1*-deficient HAP1 cells and in *NIT2*-deficient yeast. (*A*) HAP1 cell extracts were prepared from two cell lines deficient in *Nit1*, from one HAP1 cell line deficient in *Nit2* and from three control cell lines. Among these, two were cell lines that had been submitted to the CrispR/Cas9 gene inactivation procedure, but yielding no modification of the *Nit1* gene; this was done to exclude the possibility of any off-target effect of the guide RNAs used that may lead to dGSH accumulation. (*B*) WT *S. cerevisiae* and mutants lacking either scNit1 (*NIT2*-KO) (Table 1) or scNit2 (*NIT3*-KO) were cultivated in minimal defined medium with 1% glucose. Samples were collected after 15 h from starting the culture, corresponding to the late exponential growth phase. Intracellular metabolites were extracted, analyzed by LC/MS and dGSH and GSH were quantitated as above. Intracellular concentrations were calculated as detailed in *Materials and Methods*. Means ± SEM of three biological replicates are shown. A modest but statistically significant ($P < 0.05$) increase in the intracellular dGSH concentration was reproducibly observed in *NIT3*-KO cells compared with WT. The *NIT3*-KO cells appeared to accumulate substantial amounts of α-KGM (≥300 μM), and it is possible that the observed increase in dGSH is secondary to this accumulation.

accumulated to about 180 μM (i.e., at least sixfold higher than in the controls). On the other hand, GSH levels did not vary significantly between control cells and Nit1- or Nit2-deficient cells, with estimated intracellular concentrations of ∼3.5 mM in all cases (Fig. 2*A*).

We similarly found that a yeast strain deficient in the Nit1 ortholog (encoded by the *NIT2* gene) (Table 1) accumulated higher levels of dGSH than either the WT strain or the strain deleted in the Nit2 ortholog (encoded by the *NIT3* gene) (*SI Appendix*, Fig. S4*B*). For yeast, unlike for HAP1 cells, estimates of the intracellular levels of metabolites were based on direct cell volume measurements by a Multisizer 3 Coulter Counter (Beckman Coulter). The calculated intracellular concentration of dGSH reached 28 μM, whereas it was three- to sevenfold lower in the controls (Fig. 2*B*). The estimated intracellular concentration of GSH was around 0.9 mM for yeast, and did not change significantly between the KO mutant and the controls.

We also tested urine from a mouse *Nit1*-KO model (23). By LC/MS we were able to demonstrate the presence of dGSH in urine samples from these mice (Fig. 3); the concentration of dGSH assessed by this technique was 1,260 ± 130 μmol·mmol creatinine^{-1} (mean ± SEM, $n = 4$): that is, at least 15-fold higher than that observed in the controls. In fact, the concentration of dGSH in the urine of *Nit1*-KO mice was sufficiently high that it could also be detected by a spectrophotometric assay, in which the α-KG formation was measured through the coupled reactions of Nit1 and GDH, in a cuvette containing a few microliters of urine diluted in reaction buffer. The spectrophotometric assay yielded concentrations of dGSH within twofold of those estimated by LC/MS (687 ± 120 μmol·mmol creatinine^{-1}).

Gas chromatography-mass spectrometry (GC/MS) analysis of urine revealed the presence of a major peak occurring in the urine samples of all tested *Nit1*-KO mice, but almost absent from the urine of all control mice (Fig. 4 *A* and *B*). The MS spectrum of this unknown compound presented the most intense ion (presumably the molecular ion) at *m*/*z* 398. When we subjected purified dGSH to the same GC/MS analysis, we observed the appearance of a peak with the same elution time and MS spectrum (Fig. 4*C*). Analysis of the spectra indicated that this compound corresponds to a trimethylsilyl (TMS) derivative of a dehydrated, dethiolated form of dGSH, presumably generated during derivatization (Fig. 4*D* and *SI Appendix*, Fig. S5). The same *m*/*z* 398 compound was also observed in the GC/MS analysis of extracts from *Nit1*-deficient HAP1 cell lines (*SI Appendix*, Fig. S6).

Formation of dGSH Is a Side Reaction of Numerous Transaminases. The accumulation and excretion of dGSH in model systems suggests that Nit1 is the only (or at least the main) enzyme capable of metabolizing this compound. However, it remains to be established how dGSH is formed in vivo. To address this issue, we investigated the capacity of transaminases to carry out transamination reactions using GSH or OA as amino group donors. We began by focusing on glutamine transaminase K (gene symbol *KYAT1*), a rather promiscuous enzyme known to catalyze transamination reactions with glutamine, as well as with a number of other amino acids (24). Evidence that recombinant KYAT1 is also able to react with GSH is shown in *SI Appendix*, Fig. S7*A*. Addition of GSH led to a progressive change in the enzyme spectrum indicating the conversion of the protein-bound PLP cofactor to pyridoxamine 5′-phosphate. No change took place in the absence of GSH. Similar data were obtained when GSH was replaced with OA.

HPLC analysis of reaction mixtures in which OA and glyoxylate—which has the advantage of binding quite weakly to glutamine transaminase K, limiting the phenomenon of substrate inhibition observed with larger α-keto acid substrates (25, 26)—were incubated overnight with KYAT1 indicated the appearance of two peaks corresponding to dOA (*SI Appendix*, Figs. S7*B* and S8). A similar experiment performed with GSH resulted in the appearance of several peaks, corresponding to a mixture of reduced dGSH and of disulfides resulting from its reaction with GSH or with itself (*SI Appendix*, Figs. S7*C* and S9).

To measure the slow formation of dGSH and dOA by KYAT1 and by other transaminases, we used a coupled assay with Nit1 and GDH. The assay worked well in a continuous format (an example with the enzyme ornithine aminotransferase, OAT, is shown in *SI Appendix*, Fig. S10). However, to minimize artifacts because of contaminating NADH-oxidizing activities or the regeneration of L-Glu by GDH, these coupled assays were performed in a discontinuous fashion. This way we could compare the side-activities leading to dGSH to more classic activities for some representative mammalian transaminases (including both cytosolic and mitochondrial examples) (27) (Table 3). Quite remarkably, detectable activities were encountered in all cases, although they were very small compared with the more classic activities of these enzymes.

To further test whether dGSH in mammalian cells is mostly formed through aminotransferase reactions, we cultured the WT and *Nit1*-deficient HAP1 cell lines in the presence and in the absence of aminooxyacetate (AOA), which is a general inhibitor of

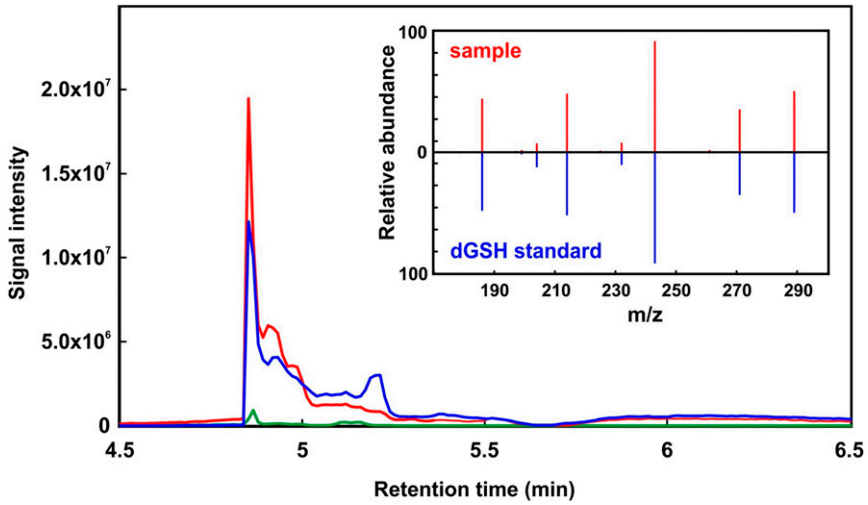

Fig. 3. LC/MS detection of dGSH in the urine of *Nit1*-deficient mice. LC/MS chromatograms showing the presence of dGSH in the urine (500-fold diluted) of a *Nit1*-KO mouse (red line) and a WT mouse (green). The blue chromatogram refers to urine from a WT mouse spiked with 25 μM purified dGSH. (*Inset*) MS2 spectrum of dGSH found in the *Nit1*-KO urine sample, mirrored with the MS2 spectrum generated from the standard.

PLP-dependent enzymes, including transaminases (28). As shown in *SI Appendix*, Fig. S11, the accumulation of dGSH in HAP1 cells decreased in a dose-dependent manner when the cells were cultivated for 24 h with 50, 100, or 200 μM AOA added to the culture medium. These data support the hypothesis that aminotransferase activity is necessary to form dGSH in vivo.

Nit1 Localizes in Both the Cytosol and the Mitochondria of Mammalian Cells. Databases indicate the existence, both in mouse and in humans, of two types of *Nit1* transcripts, which differ by their length at their 5′ end. This suggests that Nit1 can be translated from two distinct, conserved AUGs, resulting in proteins that differ by the presence (mNit1, NP_036179.1) or the absence (cNit1; NP_001229509.1) of a mitochondrial propeptide sequence. Chinese hamster ovary cells were transfected so as to express either form of the Nit1 protein fused at the C terminus to GFP. The transfected cells expressing mNit1-GFP showed localization of the protein mainly in the mitochondria but also in the cytosol, whereas those expressing cNit1-GFP showed exclusively a cytosolic localization (*SI Appendix*, Fig. S12). Overall, this double localization of Nit1 is in agreement with the results of earlier studies (23, 29) and is consistent with a role of the enzyme in recycling a side product of transaminases, which are abundant in both the cytosol and the mitochondria.

Activity of Nit1 and Nit2 Toward α-KG–CoA and Other Potential Substrates. As noted in the introduction, an alternative repair function for Nit1 could be the hydrolysis of α-KG–CoA. An enzyme capable of producing α-KG–CoA is SUGCT [the product of a gene also known as *C7orf10* (30)]. This mitochondrial enzyme reversibly exchanges CoA between a dicarboxylyl-CoA and a dicarboxylate. Its main physiological substrates are succinyl-CoA and glutarate, but in vitro it was shown to use, with lower efficiency, various other dicarboxylates, including α-KG (30).

By using the recombinant human SUGCT, we were able to produce α-KG–CoA and to show that it is hydrolyzed by mmNit1. In fact, among all dicarboxylyl-CoAs that are made by SUGCT, α-KG–CoA was found to be the best mmNit1 substrate, emphasizing that the presence of a keto function on the α-carbon is essential for substrate recognition (*SI Appendix*, Fig. S13*A*). However, mmNit2 also cleaved α-KG–CoA at almost the same rate as that observed with mmNit1 (*SI Appendix*, Fig. S13*B*), indicating that α-KG–CoA hydrolysis is not an activity unique to Nit1, unlike dGSH hydrolysis.

We also further tested the specificity of mmNit1 and of its yeast ortholog with different amides physiologically present in mammalian cells. No activity (< 0.001 μmol/min per milligram protein) was detected by measuring spectrophotometrically the formation of glutamate from L-glutamine, γ-L-glutamyl-ε-L-lysine, *N*-acetyl-aspartylglutamate, or *N*-acetylglutamate (all tested at 1-mM concentration in the presence of 500 nM enzyme). A very low activity was, however, detected with 1 mM GSH as a substrate (Table 4).

Presence of dGSH Amidases and ω-Amidases in Bacteria. BLAST searches indicated that several enteriobacteriaceae, known to contain GSH (as indicated by GSH assays or by the presence in their genomes of both GSH synthetase and γ-glutamylcysteine synthetase), contain two Nit1/Nit2 homologs. The homologs from *Escherichia coli*, *Yersinia enterocolitica*, and *Pseudomonas aeruginosa* were expressed in recombinant form and their activity toward dGSH and α-KGM was tested using a fixed concentration (80 μM) of these substrates. One of the two homologs (YafV in the case of *E. coli*) showed high activity toward α-KGM and almost no detectable activity toward dGSH, whereas the other homolog (YbeM in the case of *E. coli*) showed higher activity with dGSH than with α-KGM. The ratio of the two activities indicates that the *E. coli* enzyme is about as specific as mouse mmNit1 and scNit1, whereas the enzymes of *P. aeruginosa* (paNit1) and *Y. enterocolitica* (yeNit1) are less specific (Table 4).

Similar assays performed on the single Nit1/Nit2 homolog present in the cyanobacterium *Synechocystis*, which like other cyanobacteria contains the GSH synthesizing enzymes, indicated that it acted on both dGSH and α-KGM, with a ratio of activities of only 3.4. In contrast, the single homologs present in *Bifidobacterium longum* and in *Staphylococcus aureus*, which have no GSH synthetase, showed higher activity toward α-KGM, most particularly in the case of the *S. aureus* enzyme, which was ~3,500-fold more active with α-KGM than with dGSH (Table 4).

Remarkably, tests performed to measure glutamate formation from GSH or L-glutamine indicated that, as a rule, the "dGSH amidases" had a low but detectable activity toward GSH and no activity toward L-glutamine, while reciprocally, ω-amidases showed a low activity toward L-glutamine, but no activity toward GSH (Table 4). Thus, the side activities of these enzymes mirrored their main activities toward their physiologic, deaminated substrates.

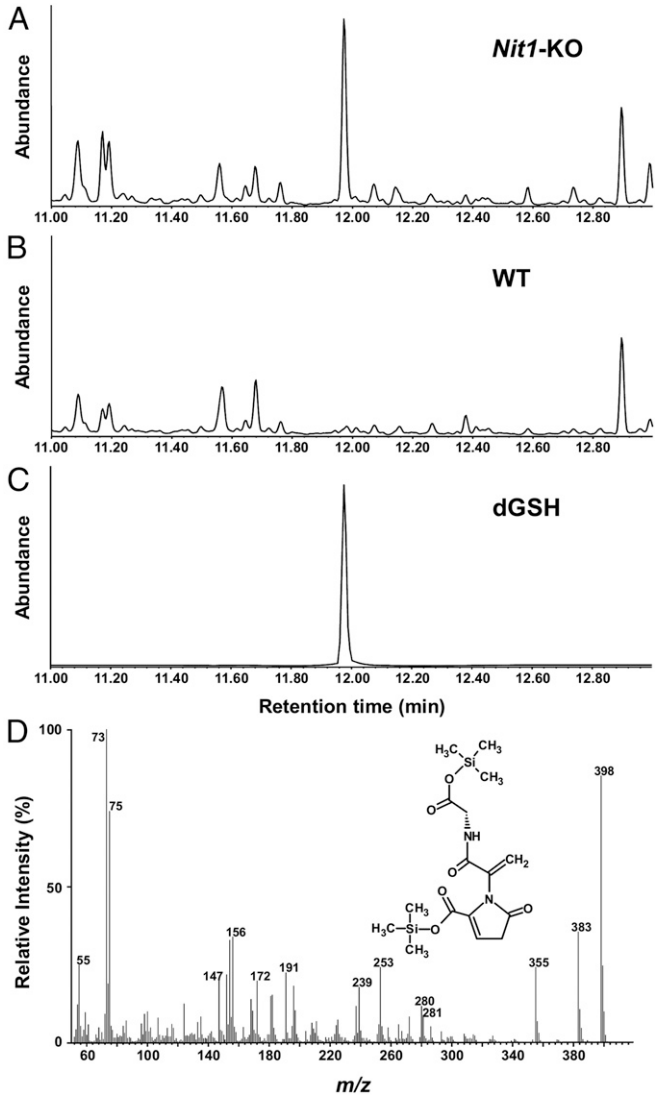

Fig. 4. GC/MS detection of a dGSH derivative in the urine of *Nit1*-deficient mice. Urine samples were treated with the TMS reagent BSFTA/TMCS [*N,O*-bis(trimethylsilyl) trifluoroacetamide-trimethylchlorosilane] (*SI Appendix, Supplementary Materials and Methods*). (*A*) GC/MS total ion current chromatogram showing the presence of a major peak (with retention time 11.97 min and *m/z* 398 for the apparent molecular ion) in the urine of a *Nit1*-KO mouse. The same peak was observed in all of the urine samples from *Nit1*-KO mice. (*B*) In contrast, the peak was undetectable in the urine of control mice. (*C*) GC/MS analysis of purified dGSH shows a peak with the same retention time and mass spectrum (see also *SI Appendix*, Fig. S5), indicating that this is a derivative of dGSH. (*D*) Mass spectrum of the compound present in the urine of *Nit1*-KO mice. The molecular ion shifted to *m/z* 416 upon silylation with *N,O*-Bis (trimethyl-d_9-silyl)acetamide (d_9-BSA) (*SI Appendix*, Fig. S5*C*), indicating that the ion is M^+ and contains two TMS moieties. High-resolution MS indicated the elemental formula $C_{16}H_{26}N_2O_6Si_2$ (exact mass 398.13892; calculated mass 398.13294; millimass error 5.98 and unsaturation of 7.0), implying for the underivatized compound MW = 254 and the elemental formula $C_{10}H_{10}N_2O_6$. The *Inset* shows the proposed structure for the dGSH derivative.

Discussion

Nit1 and Its Yeast Ortholog Hydrolyze dGSH. The role of Nit1 has remained a conundrum, despite intensive studies on this enzyme, including several structural studies (1–6, 23, 31). The results presented here are in agreement with the crystal structure of the yeast Nit1 ortholog, scNit1, which included a GSH-like molecule bound at the active site (31). The crystallized enzyme (catalytically inactivated by the replacement of Cys169 with Ala) had been expressed in *E. coli* (31), which produces GSH. The metabolite repair concept led us to consider the possibility that the substrate of Nit1 may be indeed a modified form of GSH, resulting from minor side activities of transaminases. This hypothesis has been borne out by the overall results of the present study.

The data obtained with purified recombinant enzymes show that, among the potential substrates that we tested, dGSH is by far the best for Nit1. Furthermore, our results with human *Nit1*-KO cells and with *Nit1*-KO mice indicate that dGSH is used by the mammalian Nit1 and its yeast ortholog in vivo. Because it is customary to name enzymes after their best substrate, we propose for Nit1 and its orthologs the name "dGSH amidases." This is not meant to imply that Nit1 does not act on other substrates, but these are most likely quantitatively less important than dGSH (see below). For example, the fact that mmNit1 and mmNit2 display similar activities toward α-KG–CoA, but drastically different activities toward dGSH, suggests that the evolutionary pressure allowing the conservation of Nit1 and its orthologs is based on their capacity to hydrolyze dGSH.

Structural Features Differentiating dGSH Amidases from ω-Amidases. Given their high sequence similarity, it is worthwhile to analyze the features that contribute to the substrate specificities of dGSH amidases and ω-amidases. We show in *SI Appendix*, Fig. S14*A* an alignment of all 13 amidases that have been investigated and a phylogenetic tree that was constructed from this alignment. Remarkably, the enzymes that act preferentially on dGSH and those that act preferentially on α-KGM do not generate two distinct branches (*SI Appendix*, Fig. S14*B*): the *B. longum* enzyme blYbeM acts best on α-KGM, whereas its most similar homolog, *E. coli* YbeM, hydrolyzes dGSH 500-fold better than it does with α-KGM. We noted also from pairwise sequence alignments that mouse ω-amidase (mmNit2) shows a higher degree of identity with mouse or yeast dGSH amidases (35% and 31% identity with mmNit1 and scNit1) than with its *E. coli* ortholog (26% identity with ecYafV). This finding suggests a complex evolutionary history of the Nit1/Nit2 family, where specialization toward enzymes acting as ω-amidases or dGSH amidases may have occurred more than once through convergent evolution. Such a pattern is not surprising considering the intricate history of GSH, which appears to have been "invented" on distinct occasions during evolution (32, 33).

Inspection of the alignment shows that, as expected, all 13 sequences share the catalytic triad (highlighted in yellow) typical of enzymes of the Nit1/Nit2 family (Glu45-Lys127-Cys169, according to the scNit1 numbering). Furthermore, they all share residues (highlighted in cyan) that interact with the α-KG (or oxaloacetyl) moiety of the substrates (*SI Appendix*, Fig. S15), most particularly: (*i*) an Arg residue (Arg173) located four positions after the catalytic Cys; the guanidino group of this Arg interacts with the α-carboxylic group of α-KGM or dGSH in scNit1 (31); (*ii*) a Phe or Trp (Phe195 in scNit1) ~ 25 residues downstream of the catalytic Cys; this residue interacts via π–π interaction with the keto group of α-KG in scNit1 (31), thus impeding recognition of substrates (e.g., GSH in Nit1, L-glutamine in Nit2) where the keto group is replaced by a protonated amine.

As stated in the introduction, a major discriminant between Nit1 and Nit2 is the size of the subpocket where the amido group of α-KGM is predicted to bind. This subpocket is much smaller in mmNit2 (*SI Appendix*, Fig. S15) because of the presence of Tyr87 and Tyr254 (magenta in *SI Appendix*, Fig. S15) (31). The first of these two residues is highly conserved in highly specific ω-amidases; the second residue is also conserved, if one allows for a shift of two positions in the "YafV"-type of ω-amidases (*SI Appendix*, Fig. S14*A*). We propose that these two residues are a signature for ω-amidases.

Table 3. Slow GSH transaminations carried out by five different mammalian transaminases

Enzyme	Amino group donor → Amino group acceptor (3 mM) ↓	Activity (turnovers·min^{-1}) GSH (15 mM)	L-Gln (1 mM)	L-Glu (1 mM)	L-Orn (1 mM)
KYAT1	Glyoxylate	0.17 ± 0.05	42 ± 4	<0.1	—
	4-Methylthio-2-oxobutyrate	0.049 ± 0.003	130 ± 7	<0.1	—
PSAT1	Glyoxylate	0.53 ± 0.14	1.2 ± 0.4	10 ± 2	—
	Oxaloacetate	0.17 ± 0.01	5.7 ± 0.8	23 ± 1	—
GOT1	Glyoxylate	0.018 ± 0.003	0.23 ± 0.02	0.40 ± 0.02	—
	Oxaloacetate	0.012 ± 0.002	7.8 ± 0.7	686 ± 72	—
KYAT3	Glyoxylate	0.04 ± 0.02	51 ± 3	≤0.1	—
	4-Methylthio-2-oxobutyrate	0.012 ± 0.003	25 ± 2	≤0.1	—
OAT	Glyoxylate	0.27 ± 0.06	≤0.1	5.0 ± 0.5	3.3 ± 0.2
	α-KG	—	—	—	187 ± 4

Activities are expressed as number of turnovers per active site per minute, and are the average (± SEM) of at least three separate measurements. The five recombinant transaminases examined in this table are: human glutamine transaminase K [KYAT1; the cytosolic form was tested (27)]; human phosphoserine aminotransferase (PSAT1; cytosolic); human cytosolic aspartate aminotransferase (GOT1); mouse glutamine transaminase L (KYAT3; the cytosolic form was tested); mouse ornithine aminotransferase (OAT; mitochondrial). Enzymatic assays are described in *Materials and Methods*.

Remarkably, in all dGSH amidases, the first of these two residues is replaced by a smaller residue (Ser51 in scNit1; green *SI Appendix*, Fig. S14*A*), which allows for a larger subpocket. The second residue is replaced by a basic residue (Arg250 in scNit1; green in *SI Appendix*, Fig. S14*A*), which interacts with the carboxylic group of the glycine moiety of dGSH (31). Strikingly, this basic residue is conserved in all dGSH amidases, if one allows for a one-residue shift in *E. coli* YbeM (*SI Appendix*, Fig. S14*A*); on the other hand His93, also proposed to interact with the cysteinylglycine moiety of dGSH (31) is not conserved. We therefore propose that a small residue (Gly, Ala, Ser, or Asp) in the first of the two positions and a basic residue in the second position are a signature for dGSH amidases. It is interesting to note that the first, small residue is replaced by a large, polar residue (Arg) in the *B. longum* enzyme (*SI Appendix*, Fig. S14*A*) and that this enzyme is a good ω-amidase and a poor dGSH amidase, unlike ecYbeM with which it clusters in the evolutionary tree. This finding agrees with the importance of this residue for substrate discrimination.

In *SI Appendix*, Table S3, we provide a list of ∼130 organisms with indications about their potential ability to produce GSH (as deduced from the presence of a GSH synthetase and a γ-glutamylcysteine synthetase) and the presence of dGSH amidase or ω-amidase (as deduced from similarity with the enzymes studied in the present work, combined with the presence of the signature residues described above). As summarized in Table 5, most of the organisms that we investigated have both the capacity to synthesize GSH and a putative dGSH amidase or have neither of these. Exceptions are a couple of bacteria whose genomes encode a putative dGSH amidase but no GSH synthetase, which might be because of the existence of an additional form of GSH synthetase that has not yet been identified, as was indeed proposed for *Rubrobacter xylanophilus* and *Rubrobacter radiotolerans* (34). Another exception is a significant group of species that have the capacity to synthesize GSH while not having any dGSH amidase. This finding suggests that this enzyme may be dispensed with or that a nonhomologous enzyme catalyzes the hydrolysis of dGSH in some organisms. Overall, these data indicate

Table 4. Specificity of the amidase activities of Nit1/Nit2 homologs from different bacterial species compared with the mouse and *S. cerevisiae* enzymes

Protein	dGSH amidase specific activity (μmol·min^{-1}·mg^{-1})	ω-Amidase specific activity (μmol·min^{-1}·mg^{-1})	Amidase activities: dGSH /α-KGM	Protein in assay (nM)	GSH amidase specific activity (μmol·min^{-1}·mg^{-1})	L-Glutaminase specific activity (μmol·min^{-1}·mg^{-1})
mmNit1	0.804 ± 0.042	0.002 ± 0.000	530 ± 50	10/600	0.005; 0.008	<0.001
mmNit2	<0.001	7.59 ± 0.29	<0.001	500/2	<0.001	0.003; 0.002
scNit1	8.71 ± 0.13	0.004 ± 0.000	2400 ± 35	2/600	0.003; 0.002	<0.001
scNit2	<0.001	3.59 ± 0.08	<0.001	500/2	<0.001	0.044; 0.037
ecYbeM	40.63 ± 0.27	0.178 ± 0.000	503 ± 3	2/100	0.001; 0.001	<0.001
ecYafV	0.001 ± 0.000	6.65 ± 0.08	<0.001	500/2	<0.001	0.167; 0.172
yeNit1	6.50 ± 0.17	0.20 ± 0.00	33 ± 1	10/100	0.002; 0.003	<0.001
yeYafV*	<0.001	21 ± 0.60*	<0.001	500/2	<0.001	0.002; 0.001
paNit1	13.6 ± 0.75	1.10 ± 0.10	13 ± 0.2	10/10	0.003; 0.004	<0.001
paYafV	<0.001	9.55 ± 0.08	<0.001	500/2	<0.001	0.264; 0.269
syNit1	7.77 ± 0.12	2.13 ± 0.09	3.7 ± 0.1	10/10	<0.001	<0.001
blYbeM	0.11 ± 0.00	2.44 ± 0.03	0.05 ± 0.00	100/10	<0.001	0.001; 0.000
saYafV	0.001 ± 0.000	3.87 ± 0.00	<0.001	4500/2	<0.001	0.011; 0.010

All activities were determined spectrophotometrically at 37 °C. dGSH and ω-amidase was assayed by measuring the formation of α-KG from 80 μM dGSH (column 2) or α-KGM (column 3) as described in *Materials and Methods*. The concentration of enzyme used in these assays is indicated (column 5) for dGSH amidase (first value) and ω-amidase (second value). GSH amidase and L-glutaminase activities were determined spectrophotometrically by the production of L-glutamate from 1 mM GSH or L-glutamine.

*Because of its instability at pH 8.5, all assays with this protein were performed at pH 7.2 (50 mM potassium phosphate).

Table 5. Occurrence of dGSH amidase and GSH synthetase in 133 representative organisms

GSH synthetase	dGSH amidase	No. of instances	Examples
+	+	38	*Danio rerio*, *Drosophila melanogaster*, *Arabidopsis thaliana*, and many proteobacteria and cyanobacteria
—	+	2	*Anaeromyxobacter dehalogenans*, *Salinispora arenicola*
+	—	19	*Trypanosoma brucei*, *Buchnera aphidicola*, *Xylella fastidiosa*
—	—	62	*Encephalitozoon intestinalis*, *Haemophilus influenzae*, *Haemophilus pylori*
+	Dubious	2	*Bradyrhizobium japonicum*
—	Dubious	11	*Arthrobacter alpinus*

Summary of the data presented in *SI Appendix*, Table S3, which comprises eukaryotes, eubacteria, and archaea.

that dGSH amidases are largely distributed in GSH-containing organisms, and extremely rare in others (Table 5).

Nit1 Is Useful to Correct the Unspecific Activity of Transaminases Toward GSH. GSH is one of the most abundant intracellular carriers of an α-amino group. Amino acids are usually present at much lower concentrations, except for glutamate and glutamine. It is therefore not surprising that GSH may be the subject of significant side-reactions.

Transaminases are also abundant cellular enzymes, localized mostly in the cytosol and in the mitochondria. We have tested several transaminases (both cytosolic and mitochondrial) and found that all of them possess some ability to produce dGSH. In other words, the incidental production of dGSH seems to be a feature shared by many transaminases and at least one decarboxylase (35). We use the term incidental, because the observed reaction efficiencies are remarkably small (Table 3). However, even reaction rates of such a modest order of magnitude can become very significant over time, especially when there is ample availability of substrate, as is the case for intracellular GSH.

Besides these considerations, several pieces of circumstantial evidence from model cells and animal systems support a scenario in which the formation of dGSH arises from the "mistaken" reactions of transaminases and that Nit1, by degrading dGSH, fulfills the role of a metabolite repair enzyme.

First, the observation that AOA, a general inhibitor of transaminases, limits the accumulation of dGSH is consistent with the idea that transamination is the major route for dGSH formation in vivo. In principle, dGSH could also be formed through oxidative deamination of GSH, in particular by IL4I1, the mammalian enzyme equivalent to snake venom L-amino acid oxidase. However, expression of this enzyme is exquisitely specific for cells of the immune system and is under the control of IL-4 (36), making it unlikely that IL4I1 can be a main producer of dGSH.

Second, Nit1 is found in the "right" places. We have shown that the mammalian Nit1 is located in both the cytosol and the mitochondria, the two subcellular environments where dGSH-forming transaminases are mainly localized. Additionally, expression of *Nit1* is particularly high in the liver and kidney (23), where transaminase expression is also most abundant.

Third, there is no known metabolic use for dGSH, which in fact is excreted in substantial amounts by *Nit1*-KO mice. In contrast, the products of the Nit1 reaction (α-KG and cysteinylglycine) are readily metabolized (37). These observations are consistent with dGSH representing a "waste" compound, which may require a repair enzyme to be recycled into metabolites useful for the cell.

In principle, transaminations where GSH is the amino group donor could afford the same advantage as transaminations with glutamine. In fact, both processes are essentially irreversible, because the products that are formed cyclize and because they are hydrolyzed by an amidase: Nit2 (in the case of α-KGM) or Nit1 (in the case of dGSH). The metabolic disadvantage of the pathway involving GSH is that resynthesizing GSH from dGSH would cost two ATP molecules compared with one for regenerating glutamine through the glutamine synthase reaction. Furthermore, if transamination reactions with GSH were highly active, the intracellular levels of cysteinylglycine and of its hydrolysis product cysteine might rise substantially. Because cysteine is more reactive and more toxic than is GSH (38), this would represent a liability for the cell.

There has obviously been a counter-selection during evolution to avoid GSH being used as a standard substrate for transamination. Nevertheless, the very presence of Nit1, which can "correct" the formation of dGSH, may conceivably limit the evolutionary pressure for transaminases to achieve an even greater discrimination against GSH, potentially explaining why so many enzymes retain some marginal ability to form dGSH.

It is likely that transaminases catalyze side reactions toward other γ-glutamyl-amino acids or γ-glutamyl-amines that are formed by transglutamylation reactions using GSH as a donor (39). It would be interesting to determine whether the variety of α-KG derivatives that might be formed in this way is processed by Nit1 and its functional orthologs. However, given the abundance of GSH, it is likely that these other potential derivatives are only of minor importance.

Considerations Concerning the Biological Importance of Nit1. The present work establishes a clear link between Nit1 enzyme activity and the metabolism of GSH. The distribution of Nit1 orthologs in disparate (but GSH-producing) organisms attests to the biological importance of the dGSH amidase function and strongly implies that this function provides significant selective advantages. On the other hand, both Nit1-deficient cells and mice do not show any dramatic phenotype, raising the question as to what these advantages can be.

GSH has many recognized functions (40): these include roles as an antioxidant (and as a cofactor for the neutralization of peroxides and related products generated by reactive oxygen species), in the detoxification of xenobiotics, in metal homeostasis, and as a preferred form of cysteine storage and transport. In effect, GSH can be regarded as a "protected," more stable form of cysteine (e.g., less prone to autooxidation) (41).

An obvious advantage of having a dGSH amidase is therefore to avoid the loss of GSH (and hence of L-cysteine); this can be best appreciated by considering the case of the mammalian enzyme. If the levels of dGSH excretion observed in mice (we consider here the lowest estimate, 687 μmol·mmol creatinine^{-1}) were applicable to humans, a 70-kg individual deficient in *Nit1* would excrete daily about 2.2 g of GSH as dGSH. Such an amount corresponds to ∼15% of total body GSH. By comparison, individuals with γ-glutamyl transpeptidase deficiency were reported to eliminate in urine up to 1 g GSH per day (42).

Given the high rate at which GSH is turned over, this drain of GSH may be overcome and cause no harm under most conditions. Indeed, the accumulation of dGSH in *Nit1*-KO cell models does not appear to significantly affect the GSH levels in the same cells (Fig. 2). However, it seems reasonable to hypothesize that the depletion of GSH may be less sustainable in cells particularly rich in transaminases or in times when the GSH demand is high. In addition to this hypothesis, the accumulation of dGSH might also subtly alter some cellular functions. For example, because there are many enzymes (including oxidoreductases and glutathione

S-transferases) that use GSH as a substrate, dGSH may potentially interfere with the function of at least some of them. In the long term, these phenomena may represent a sizable selective disadvantage for the Nit1-deficient organisms.

Nit1 was classified as a tumor suppressor because of its association with the fragile histidine-triad protein Fhit. In fact, whereas Nit1 and Fhit are discrete proteins in mammals, they are expressed as fused domains in widely distant invertebrates such as nematodes, insects, arthropods, and flatworms (2, 23). Fhit proteins act best to hydrolyze adenyl-derivatives, such as ApppA and AppppA (1, 2). However, we do not see any obvious connection between the enzymic functions of Fhit and of Nit1. We must also stress that, although data collected in mammalian cells, mice models, and human samples suggest that Nit1 promotes apoptosis (23) and affects, in a complex fashion, the development and progression of some types of tumors (23, 43), it is uncertain whether these roles bear any connection with the enzyme's catalytic function. In fact, mutation of the conserved active site cysteine to an alanine did not alter the ability of Nit1 to promote apoptosis in human cells (23). Perhaps related to the above, a recent study reported that Nit1 can interact with β-catenin, repressing β-catenin–mediated transcription, and that this repressive activity is not affected by mutation of the catalytic cysteine (44). It is therefore possible that the Fhit–Nit1 connection may reflect other (as yet unclearly defined) Nit1 functions that do not depend on the catalytic hydrolysis of dGSH.

Concluding Remarks

The results presented here establish Nit1 as a new example of a highly conserved enzyme with a metabolite repair role. Further work will be needed to understand why the dGSH amidase activity of Nit1 is important. Is it because dGSH exerts some toxic effects in the cells or is it to recycle precious building blocks? In any case, this work suggests that, when addressing the function of the numerous putative enzymes encoded by the human and other genomes, their possible involvement in metabolite repair should be seriously considered. The enormous chemical diversity that side reactions add to the metabolome makes this search for enzymic function both more challenging and more interesting.

Materials and Methods

Materials and other methods used in this work are mainly provided in the *SI Appendix*. All procedures involving mice were performed following protocols approved by the Ohio State University Institutional Animal Care and Use Committee.

Cloning, Overexpression, and Purification of Recombinant Proteins. His_6-tagged (mouse) mmNit1 (lacking the targeting peptide sequence) and mmNit2 were expressed as reported earlier (5). The human cytosolic transaminases, glutamine transaminase K (KYAT1; previously CCBL1), aspartate aminotransferase (GOT1), and phosphoserine aminotransferase (PSAT1) were expressed as described previously (25). The coding sequences of the yeast Nit1 and Nit2 orthologs (encoded by the *NIT2* and *NIT3* genes, respectively), and of the bacterial homologs shown in Table 1, with the exception of ecYafV and blYbeM, were PCR-amplified from genomic DNA, cloned in the pET28a vector, and expressed as recombinant proteins (N-terminal His6 tag) in *E. coli* BL21(DE) cells. ecYafV was expressed from an ASKA clone (45) and blYbeM was produced using a pET28A plasmid containing a codon optimized synthetic sequence (GenScript). The coding sequences of mouse ornithine transaminase (OAT) and glutamine transaminase L (official gene symbol KYAT3; previously CCBL2) were PCR-amplified from mouse cDNA and cloned into expression vectors (pET28a and pET24, respectively); the proteins were then expressed in recombinant form in *E. coli* BL21(DE) cells. Details of (*i*) the primers used for PCR amplification, (*ii*) the restriction enzymes used for cloning, and (*iii*) the culture conditions adopted for the overexpression of individual proteins are provided in *SI Appendix, Supplementary Materials and Methods*. Preparation of bacterial homogenates and purification of recombinant proteins by metal-affinity chromatography (HisTrap columns) were carried out as previously described (46). Purified proteins were finally kept in 25 mM Hepes, pH 7.2, 300 mM NaCl, 1 mM DTT, and 10% (vol/vol) glycerol, and stored at −70 °C until use.

Production of HAP1 Cell Lines Deficient in Nit1 and Nit2 by CRISPR/Cas9. The human-derived HAP1 cell line (Horizon Discovery) expresses both the *Nit1* and the *Nit2* genes, as described by the number of transcripts per kilobase million for Nit1 (13.85; https://www.horizondiscovery.com/human-nit1-knockout-cell-line-hzghc4817) and for Nit2 (53.21; https://www.horizondiscovery.com/human-nit2-knockout-cell-line-hzghc56954). The parental cells were therefore used to create HAP1 cell lines deficient in either Nit1 or Nit2 by the CRISPR/Cas9 technology (details provided in *SI Appendix, Supplementary Materials and Methods*).

The clones we ultimately selected for further studies presented the following modifications in the *Nit1* or *Nit2* genes: for Nit1-T1, a 13-bp deletion, leading to a change in reading frame after the codon for Val-71 and a premature stop 18 codons later; for Nit1-T2, a >190-bp insertion after the codon for Asn179, which also leads to a premature stop after about 40 codons; finally, for NIT2, an 80-bp insertion after Glu64, with a premature stop after 20 codons.

Preparation of Amidase Substrates. α-KGM was prepared by oxidation of L-glutamine by snake venom L-amino acid oxidase, as previously described (5). dGSH and dOA were prepared by an analogous procedure. Briefly, a 200-mM solution of GSH or OA, adjusted to pH 7, was incubated overnight at 37 °C under agitation with 4 units/mL of catalase and 2 mg/mL of *Crotalus adamanteus* L-amino acid oxidase (Sigma). After incubation, the reaction mixture for the preparation of dGSH was usually supplemented with solid DTT (~120 mM final) to reduce the disulfide adducts. The mixture was then deproteinized by addition of $HClO_4$ to a final concentration of 3% and centrifuged at 15,000 × *g* for 15 min at 4 °C. A first purification of the products from reagents was accomplished by applying the supernatant to a 5 mL AG50 cation-exchange column, equilibrated with 0.1 M HCl. The eluate was neutralized with 3 M K_2CO_3, and the $KClO_4$ precipitate was removed by centrifugation. dGSH and dOA were further purified by HPLC from a 19 × 150 mm XBridge Prep C18 column (Waters), by isocratic elution with 3% aqueous acetonitrile/0.1% trifluoroacetic acid at a flow rate of 20 mL/min. Both reduced dGSH (*m/z* 307, detected as $[MH]^+$) and dOA (*m/z* 289) eluted in two adjacent peaks of similar areas, attributable to the two anomeric forms of the cyclized ketoacids. This finding was supported by the observation that the compounds in both peaks were substrates for Nit1.

ω-Amidase Assay. The reaction of mmNit2 and its orthologs was monitored through a coupled assay with GDH (5). Measurement of this reaction is complicated by the fact that α-KGM essentially exists in cyclic forms, which at equilibrium are about 300 times more abundant than the linear form. The rate of equilibration between the cyclic and linear structure is pH-dependent, being faster at alkaline pH. As only the open form appears to be a substrate for mmNit2 (5, 20), the ω-amidase reaction was measured at pH 8.5 and using very diluted enzyme (1–2 nM). The reaction mixture (1-mL final volume) contained 50 mM Bicine (pH 8.5), 50 mM KCl, 0.5 mg/mL BSA, 2 mM DTT, 0.22 mM NADH, 5 mM ammonium acetate, 2.4 units/mL GDH, as well as the amidase. These assays were performed at 30 °C (results shown in Table 2) or 37 °C (results shown in Table 4). Under these conditions, the measured activity increased linearly with ω-amidase concentration, indicating that the reaction was not rate-limited by opening of the cyclic form of α-KGM. The range of α-KGM concentrations tested was 40–1,500 μM.

dGSH Amidase Assay. Release of α-KG from dGSH and dOA by Nit1 and its orthologs was measured through a coupled assay with GDH, analogous to the ω-amidase assay. The reaction mixture (1 mL) contained 50 mM buffer (Bicine or Hepes), 50 mM KCl, 0.5 mg/mL BSA, 2 mM DTT, 0.22 mM NADH, 5 mM ammonium acetate and 2.4 units/mL GDH. These assays were performed at 30 °C (results shown in Table 2) or 37 °C (results shown in Table 4). When these reactions were performed to determine the enzyme catalytic parameters with dGSH, the buffer used was Bicine pH 8.5 and the concentration of the amidase enzyme was maintained in the range 10–40 nM (mmNit1) or 10–20 nM (scNit1). Under these conditions, the measured activity depended linearly on amidase concentration, indicating that the process was not rate-limited by opening of the cyclic form of the substrate. The range of dGSH concentrations tested was 15–330 μM.

GSH and Other Transamination Assays. Transaminases (1–5 μM) were incubated for up to 24 h at 30 °C, in the presence of GSH (5 or 15 mM) and of an appropriate amino group acceptor in 50 mM Bicine buffer pH 8.5, 50 mM KCl, 0.5 mg/mL BSA, 2 mM DTT. The final volume of the reaction mixture was

typically 0.6 mL. At given times, aliquots (120 μL) were taken from the reaction mixture and heated at 100 °C for 5 min to stop the reaction. The protein precipitate was removed by centrifugation and the content of dGSH in the aliquot was assessed spectrophotometrically through the coupled Nit1-GDH assay described above. Other transaminase assays shown in Table 3 are described in *SI Appendix, Supplementary Materials and Methods*.

Other Specificity Assays. The GSH amidase and the L-glutaminase activities of all amidases (shown in Table 4) were tested in the presence of 1 mM substrate by measuring spectrophotometrically at 37 °C the formation of glutamate. The reaction mixture (1-mL final volume) contained 50 mM Bicine (pH 8.5), 50 mM KCl, 0.5 mg/mL BSA, 2 mM DTT, 0.2 mM NAD^+, 0.5 mM ADP-Mg, 3.5 units/mL GDH, as well as the amidase (100–500 nM). The amidase activity (glutamate producing) of mmNit1 and scNit1 (500 nM in the assay) toward 1 mM γ-L-glutamyl-ε-L-lysine, *N*-acetyl-aspartylglutamate or *N*-acetylglutamate was tested using the same assay.

LC/MS Analyses. Full scans (307–312 *m/z*) for monoisotopic mass detection and natural isotope distribution, selected ion monitoring (307.06 *m/z* and 308.09 *m/z* for dGSH and GSH, respectively, using a measurement window of 0.5 *m/z*) for absolute and relative quantification, and parallel reaction monitoring (307.06 *m/z* and 308.09 *m/z* parent ions, respectively, detecting 50–300 *m/z* fragments) were performed on all samples in separate runs. Standards were prepared in a matrix as close to the samples as possible. For the analysis of yeast and mammalian cell extracts, standard curves of GSH and dGSH were prepared in LC/MS grade water:MeOH (50:50). For the analysis of mouse urine, dGSH standard curves were prepared in urine from a WT mouse. Details on the instrument used, type of column, and separation protocols for GSH and dGSH determination are provided in *SI Appendix, Supplementary Materials and Methods*.

ACKNOWLEDGMENTS. We thank Drs. Yoshito Inoue and Morimasa Ohse (Kanazawa Medical University) and Mrs. Nathalie Chevalier (de Duve Institute, Université Catholique de Louvain) for excellent technical assistance, and Dr. Juliette Létoquart (de Duve Institute) for her help in the preparation of *SI Appendix*, Fig. S15. The E.V.S. laboratory is supported by a WELBIO grant of the Walloon Region, by the Fonds de la Recherche Scientifique Médicale, by the Belgian National Lottery, and by the Interuniversity Attraction Poles Programme initiated by the Belgian Science Policy Office (Grant P7/43 to E.V.S.). M.V.d.-C. and G.T.B. are "Chercheurs qualifié" of the Fonds National de la Recherche Scientifique. The C.L.L. laboratory is supported by the Fonds National de la Recherche Luxembourg Grants CORE C13/BM/5773107 and AFR-PDR (Aides à la Formation-Recherche postdoctoral research) 9180195 (to K.W.E.).

1. Pekarsky Y, et al. (1998) Nitrilase and Fhit homologs are encoded as fusion proteins in *Drosophila melanogaster* and *Caenorhabditis elegans*. *Proc Natl Acad Sci USA* 95: 8744–8749.
2. Pace HC, et al. (2000) Crystal structure of the worm NitFhit Rosetta Stone protein reveals a Nit tetramer binding two Fhit dimers. *Curr Biol* 10:907–917.
3. Barglow KT, Cravatt BF (2006) Substrate mimicry in an activity-based probe that targets the nitrilase family of enzymes. *Angew Chem Int Ed Engl* 45:7408–7411.
4. Barglow KT, et al. (2008) Functional proteomic and structural insights into molecular recognition in the nitrilase family enzymes. *Biochemistry* 47:13514–13523.
5. Jaisson S, Veiga-da-Cunha M, Van Schaftingen E (2009) Molecular identification of omega-amidase, the enzyme that is functionally coupled with glutamine transaminases, as the putative tumor suppressor Nit2. *Biochimie* 91:1066–1071.
6. Krasnikov BF, et al. (2009) Identification of the putative tumor suppressor Nit2 as omega-amidase, an enzyme metabolically linked to glutamine and asparagine transamination. *Biochimie* 91:1072–1080.
7. Meister A, Levintow L, Greenfield RE, Abendschein PA (1955) Hydrolysis and transfer reactions catalyzed by omega-amidase preparations. *J Biol Chem* 215:441–460.
8. Cooper AJ, Meister A (1977) The glutamine transaminase-omega-amidase pathway. *CRC Crit Rev Biochem* 4:281–303.
9. Cooper AJ, et al. (2016) ω-Amidase: An underappreciated, but important enzyme in L-glutamine and L-asparagine metabolism; relevance to sulfur and nitrogen metabolism, tumor biology and hyperammonemic diseases. *Amino Acids* 48:1–20; erratum in 2015, *Amino Acids* 47:2671–2672.
10. Galperin MY, Koonin EV (2004) 'Conserved hypothetical' proteins: Prioritization of targets for experimental study. *Nucleic Acids Res* 32:5452–5463.
11. Galperin MY, Koonin EV (2010) From complete genome sequence to "complete" understanding? *Trends Biotechnol* 28:398–406.
12. Linster CL, Van Schaftingen E, Hanson AD (2013) Metabolite damage and its repair or pre-emption. *Nat Chem Biol* 9:72–80.
13. Van Schaftingen E, et al. (2013) Metabolite proofreading, a neglected aspect of intermediary metabolism. *J Inherit Metab Dis* 36:427–434.
14. Rzem R, et al. (2004) A gene encoding a putative FAD-dependent L-2-hydroxyglutarate dehydrogenase is mutated in L-2-hydroxyglutaric aciduria. *Proc Natl Acad Sci USA* 101: 16849–16854.
15. Van Schaftingen E, Rzem R, Veiga-da-Cunha M (2009) L-2-Hydroxyglutaric aciduria, a disorder of metabolite repair. *J Inherit Metab Dis* 32:135–142.
16. Collard F, et al. (2016) A conserved phosphatase destroys toxic glycolytic side products in mammals and yeast. *Nat Chem Biol* 12:601–607.
17. Gerlt JA, et al. (2011) The enzyme function initiative. *Biochemistry* 50:9950–9962.
18. Meister A (1953) Preparation and enzymatic reactions of the keto analogues of asparagine and glutamine. *J Biol Chem* 200:571–589.
19. Meister A, Otani TT (1957) Omega-amide and omega-amino acid derivatives of alpha-ketoglutaric and oxalacetic acids. *J Biol Chem* 224:137–148.
20. Hersh LB (1971) Rat liver omega-amidase. Purification and properties. *Biochemistry* 10:2884–2891.
21. Buell MV, Hansen RE (1960) Reaction of pyridoxal-5-phosphate with aminothiols. *J Am Chem Soc* 82:6042–6049.
22. Bar-Even A, et al. (2011) The moderately efficient enzyme: Evolutionary and physicochemical trends shaping enzyme parameters. *Biochemistry* 50:4402–4410.
23. Semba S, et al. (2006) Biological functions of mammalian Nit1, the counterpart of the invertebrate NitFhit Rosetta stone protein, a possible tumor suppressor. *J Biol Chem* 281:28244–28253.
24. Cooper AJ, et al. (2008) Substrate specificity of human glutamine transaminase K as an aminotransferase and as a cysteine S-conjugate β-lyase. *Arch Biochem Biophys* 474: 72–81.
25. Donini S, et al. (2009) Recombinant production of eight human cytosolic aminotransferases and assessment of their potential involvement in glyoxylate metabolism. *Biochem J* 422:265–272.
26. Schiroli D, Peracchi A (2015) A subfamily of PLP-dependent enzymes specialized in handling terminal amines. *Biochim Biophys Acta* 1854:1200–1211.
27. Malherbe P, Alberati-Giani D, Kohler C, Cesura AM (1995) Identification of a mitochondrial form of kynurenine aminotransferase/glutamine transaminase K from rat brain. *FEBS Lett* 367:141–144.
28. Korangath P, et al. (2015) Targeting glutamine metabolism in breast cancer with aminooxyacetate. *Clin Cancer Res* 21:3263–3273.
29. Sun J, et al. (2009) Nit1 and Fhit tumor suppressor activities are additive. *J Cell Biochem* 107:1097–1106.
30. Marlaire S, Van Schaftingen E, Veiga-da-Cunha M (2014) C7orf10 encodes succinate-hydroxymethylglutarate CoA-transferase, the enzyme that converts glutarate to glutaryl-CoA. *J Inherit Metab Dis* 37:13–19.
31. Liu H, et al. (2013) Structures of enzyme-intermediate complexes of yeast Nit2: Insights into its catalytic mechanism and different substrate specificity compared with mammalian Nit2. *Acta Crystallogr D Biol Crystallogr* 69:1470–1481.
32. Copley SD, Dhillon JK (2002) Lateral gene transfer and parallel evolution in the history of glutathione biosynthesis genes. *Genome Biol* 3:research0025.
33. Fahey RC (2013) Glutathione analogs in prokaryotes. *Biochim Biophys Acta* 1830: 3182–3198.
34. Johnson T, Newton GL, Fahey RC, Rawat M (2009) Unusual production of glutathione in Actinobacteria. *Arch Microbiol* 191:89–93.
35. Novogrodsky A, Meister A (1964) Control of aspartate beta-decarboxylase activity by transamination. *J Biol Chem* 239:879–888.
36. Mason JM, et al. (2004) IL-4-induced gene-1 is a leukocyte L-amino acid oxidase with an unusual acidic pH preference and lysosomal localization. *J Immunol* 173: 4561–4567.
37. Josch C, Klotz LO, Sies H (2003) Identification of cytosolic leucyl aminopeptidase (EC 3.4.11.1) as the major cysteinylglycine-hydrolysing activity in rat liver. *Biol Chem* 384: 213–218.
38. Cooper AJ (1997) Glutathione in the brain: Disorders of glutathione metabolism. *The Molecular and Genetic Basis of Neurological Disease*, eds Rosenberg R, Prusiner S, DiMauro S, Barchi R (Butterworth-Heinemann, Boston), 2nd Ed, pp 1195–1230.
39. Keillor JW, Castonguay R, Lherbet C (2005) Gamma-glutamyl transpeptidase substrate specificity and catalytic mechanism. *Methods Enzymol* 401:449–467.
40. Aoyama K, Watabe M, Nakaki T (2008) Regulation of neuronal glutathione synthesis. *J Pharmacol Sci* 108:227–238.
41. delCardayre SB, Stock KP, Newton GL, Fahey RC, Davies JE (1998) Coenzyme A disulfide reductase, the primary low molecular weight disulfide reductase from *Staphylococcus aureus*. Purification and characterization of the native enzyme. *J Biol Chem* 273:5744–5751.
42. Griffith OW, Meister A (1980) Excretion of cysteine and gamma-glutamylcysteine moieties in human and experimental animal gamma-glutamyl transpeptidase deficiency. *Proc Natl Acad Sci USA* 77:3384–3387.
43. Wang YA, et al. (2016) Nitrilase 1 modulates lung tumor progression in vitro and in vivo. *Oncotarget* 7:21381–21392.
44. Mittag S, et al. (2016) A novel role for the tumour suppressor Nitrilase1 modulating the Wnt/β-catenin signalling pathway. *Cell Discovery* 2:15039.
45. Kitagawa M, et al. (2005) Complete set of ORF clones of *Escherichia coli* ASKA library (a complete set of *E. coli* K-12 ORF archive): Unique resources for biological research. *DNA Res* 12:291–299.
46. Gemayel R, et al. (2007) Many fructosamine 3-kinase homologues in bacteria are ribulosamine/erythrulosamine 3-kinases potentially involved in protein deglycation. *FEBS J* 274:4360–4374.